Experiment and theoretical analysis of electromagnetic interference on communication systems in multi-rails environment

Received 20 April 2022
Revised 11 May 2022
Accepted 11 May 2022

Xuwei Jin
China Railway Eryuan Engineering Group Co. Ltd., Chengdu, China, and
Shize Huang, Xiaowen Liu, Jing Zhou, Jinzhe Qin, Decun Dong and Xingying Li
Tongji University, Shanghai, China

Abstract

Purpose – Electromagnetic interference (EMI) on communication systems of unban rail transit can hardly be clarified because of complicated factors around railways. This paper aims to target this issue and extend experimental and theoretical analysis.

Design/methodology/approach – This paper take the Nanjing Dashengguan Bridge as an example, because it carries the most tracks in the world and bears three kinds of trains running through, providing a perfect complex environment. First, it investigates the three communication systems, terrestrial trunked radio, communications-based train control (CBTC) and passenger information system (PIS) that Nanjing Metro uses, and select appropriate devices accordingly. Second, it establishes a system level platform and conduct three tests to analyze their respective operating principles and performance difference under common electromagnetic environments. Third, it adopts theoretical formula to verify test results.

Findings – The experiment results and theoretical analysis mutually corroborate each other and present practical recommendations: an 8 m or more distance between two tracks will ensure no obvious EMI created by a passing train on communication systems; two certain communication systems should not share the same frequency band; interference level is more related to field strength than weathers and building materials; and CBTC DSSS waveguide mode as well as PIS LTE mode are preferred.

Originality/value – This research also provides a practical method of investigating EMI for other complex situations.

Keywords Electromagnetic interference, Multirails, System level EMC test, AP access point, Communication mode

Paper type Research paper

This research is supported by the National Natural Science Foundation of China (61703308), the Sichuan Science and Technology Program (2019YFG0040), the National Key R&D Program of China (2016YFB1200402) and the Fundamental Research Funds for the Central Universities. The authors are grateful to the reviewers' helpful comments and suggestions.

Smart and Resilient Transport
Vol. 4 No. 2, 2022
pp. 134-154
Emerald Publishing Limited
e-ISSN: 2632-0495
p-ISSN: 2632-0487
DOI 10.1108/SRT-03-2022-0002

1. Introduction

China's high-speed rails have expanded at a world-leading pace for more than a decade, along with the progress of metros and other kinds of passenger rails. Chances are high that different kinds of transit trains are running on adjacent tracks, and create complex electromagnetic environments that may interfere with their respective communication systems (Flyvbjerg *et al.*, 2005; Flyvbjerg *et al.*, 2007).

A typical example is Nanjing Dashengguan Yangtze River Bridge, which carries the most railway lines in the world. It bears six tracks: two for the Beijing–Shanghai High-Speed Railway, two for the Shanghai–Wuhan–Chengdu Railway and two for the Ninghe Intercity Transit (part of the Nanjing Metro). The electromagnetic influences on urban rail transit communication systems when three kinds of trains converge, however, have yet to be clarified, and particular factors that function in system performance need to be identified (Heddebaut *et al.*, 2017).

Therefore, this research intends to establish an experimental method that can effectively acquire operating characteristics of main communication systems under various external environments, so that direct influence factors such as line distance and weather condition will be explicit. We can monitor performance degradation in certain situations. Then, whether mode adjustment will improve work status and whether cochannel interference is severe, can be analyzed in detail.

1.1 Prior research

Many researchers have noticed electromagnetic interferences (EMI) around railways and explored different ways to detect them. This paragraph reviews relevant experiments that make an assessment of communication quality to understand widely used experimental facilities as well as design principles. Jun *et al.* (2016) invested EMI of 350 km h^{-1} China Standard Electric Multiple Units. They used a quasi-peak detector in receiver and spectrum analyzer to find out whether interference values of nine commonly occupied frequency bands were within the specified range under static and dynamic conditions. The group also found that the traction system was the main EMI source. Xiwei and Feng (2014) targeted Wuhan–Guangzhou high-speed railway and proposed a more practical resolution bandwidth to obtain the railways' EMI from 30 MHz to 1 GHz. Both concerned about standard optimization as well as external interference recognition. Xing Kui *et al.* (2015) introduced a rapid interference response test for receiver that used automatic dual-frequency test system. Pous *et al.* (2018) further proposed a full-time EMI measurement system, which could increase measuring time and reduce environmental noise to obtain the most accurate measuring results. Although these attempts all reached satisfying results, their experimental methods and instruments were simple and results were far from enough. In addition to external interference monitor, researchers put effort into finding out the primary factor among various mobile communication systems. Ahmad *et al.* (2017), for example, designed a cooperative communication scheme to analyze coexistence of passenger information system (PIS)-LTE and LTE-R networks, where indicators such as receiving interference and outage probability were selected to evaluate performance under particular scenarios. They verified that cochannel interference was a common occurrence for high-speed railways, because the communication systems occupy relatively stable frequency bands. Although involved experimental methods can be used for reference, specific equipment installation is extremely difficult to come true, especially for urban rail transits, which lack prior research.

Actually, many researchers have also examined electromagnetic influences on communication systems in theoretical ways. It is convenient to think that communication mainly involves signal processing. For example, Zhang *et al.* (2018) established a magnetic interference calculation model for signal cable, which was verified by EMI tests on single- and double-ended cables. Li Wei *et al.* (2017) established two EMI prediction models and took different communication devices as objects to explain their effectiveness. However, they only considered ideal testing environment and ignored such condition that different communication systems enabled at the same time. Hence, numerical calculation with simplified experimental verification cannot meet the increasing needs.

Unfortunately, no experimental scheme can yet detect communication faults in complex environments, such as different trains running on close tracks. Nevertheless, we intend to set up one-to-one scale experimental facilities and innovate systematic procedures, so that the cause of diverse issues which emerge under above circumstances can be described. In detail, we are responsible for large-scale project design and drawing after confirming Ninghe Intercity Transit as objective. Concerning about engineering guidance, we determine system performance reference index, such as RSSI for communications-based train control (CBTC). Then, meaningful conclusions can be arrived at based on our research. For higher reference value, we propose universally applicable improvement measures. Except for band occupancy, mode selection is also one of the focuses. We learned from existing studies and carried out the experiment between CBTC and PIS, communication systems of urban rail transits, resulting in more comprehensive feedback.

In summary, real data from this study demonstrates the reliability of communication engineering, and moreover, supports the technological development in the field of urban rail transit electromagnetic compatibility.

1.2 Background on the Nanjing Dashengguan Yangtze River Bridge

As typical landmark in railway construction, Dashengguan Yangtze River Bridge sets a successful record for long-span bridges with multiple railway tracks. To improve integrity and smoothness of the bridge structure, the composite slab-truss structure is of the priority. It is also the first attempt that Q420qE structural steel was applied in the bridge. However, whether the material has obvious influence on electromagnetic components of communication systems needs to be further studied.

As shown in Figure 1, the up- and downlink of Ninghe Intercity Transit are, respectively, 8.2 and 8.7 m far from Beijing–Shanghai High-Speed Railway and Shanghai–Wuhan–Chengdu Railway (Mingyang, 2017). Alternating current (AC)- and direct current (DC)-electrified railways are close than ever before, which may give rise to dangerous voltage on urban rail transit traction network through electromagnetic induction. Therefore, we choose Ninghe Intercity Transit as the experimental subject and launch field experiment which basically covers main communication systems of it. And through performance comparison, relevant departments can find out the most possible interference cause and consequence from diverse disturbance sources.

However, sophisticated equipment build process is one of the technological difficulties that nobody has conquered so far, but our experimental scheme is perfect enough to analyze almost all EMI problems on the selected objective. Other research teams can later use the paper for reference to draw broad conclusions.

2. Technology roadmap and experiment setup

2.1 Technology roadmap

Figure 2 explains our approach that combines theoretical and experimental analysis.

Three systems are selected at the stage of object refinement, for a daily operation of Nanjing Metro needs three kinds of services using radio communications: terrestrial trunked

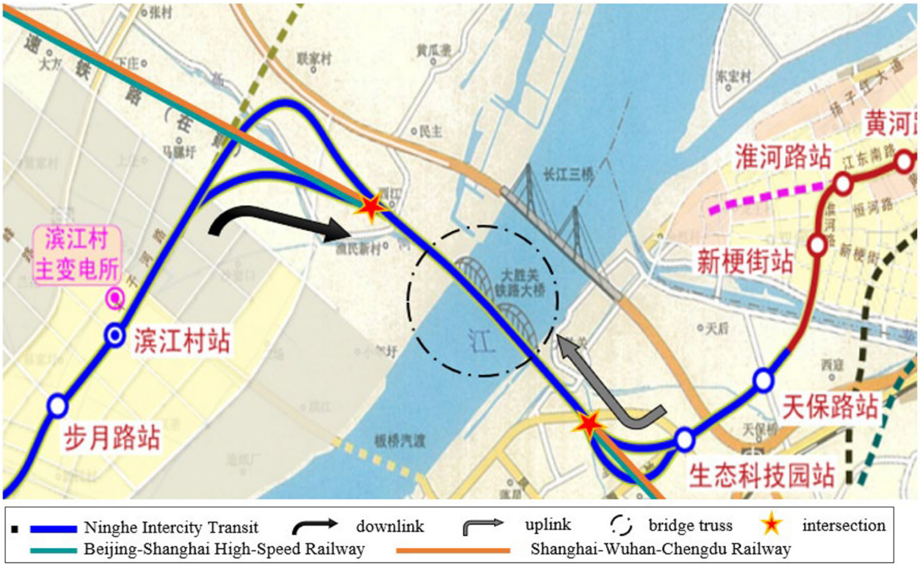

Figure 1. Satellite image of tracks on Nanjing Dashengguan Yangtze River Bridge, which is taken from Baidu Map

radio (TETRA) for command and dispatch service, CBTC, a railway signaling system and PIS providing public transport information (Peng, 2015), as illustrated in Table 1.

Normally, the three systems work within their respective frequency bands, but signal transmissions malfunction sometime due to external EMI. Thus, we deployed our experiment and analysis to figure out to what extent signal transmissions is affected under different conditions.

2.2 External interference test

To learn how the three communication systems normally work, the interference test was conducted in outer space. Figure 3 depicts the connectivity among main equipment.

Antenna input was considered as some degree of interference, which could be calculated by spectrum analyzer. Sometimes low noise amplifier or attenuator was necessary to get more effective data. Then we obtained related parameters such as antenna gain and feeder loss provided by EMI measurement receiver.

We chose seven test points, the distribution of which is exhibited in Figure 4. Points 1–5 were set along the Shanghai–Wuhan–Chengdu Railway every 500 m, while points 6 and 7 on the Beijing–Shanghai high-speed side. However, among them, points 5 and 7 were on the concrete part of the bridge, whereas others on the steel part. Thus, we could pinpoint the main influence factors. Besides, for better accuracy, test duration at every point should be no less than 30 min.

2.3 Interference comparison test

We conjecture that AC carried by Beijing–Shanghai High-Speed Railway (Figure 5) would affect DC traction device of Ninghe Intercity Transit. Hence, the same test was conducted as comparison group when tracks of Beijing–Shanghai High-Speed Railway and Ninghe Intercity Transit converged.

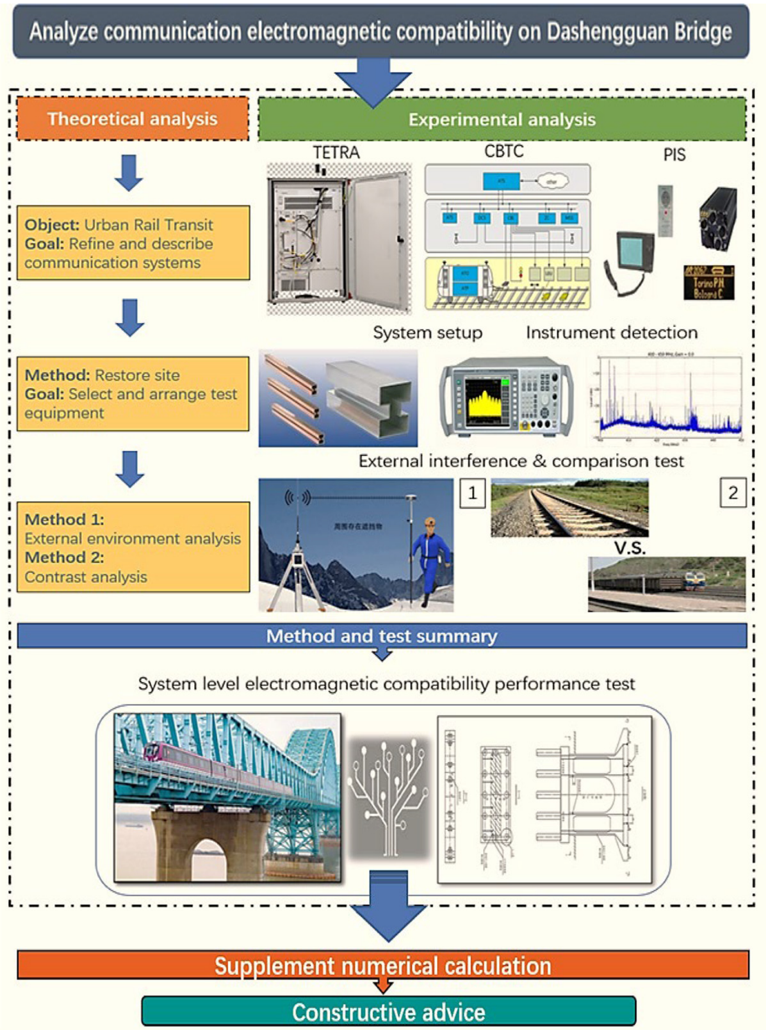

Figure 2.
Technology roadmap

Table 1.
The three commonly used metro communication systems

Item	Main function	Transmission channel	Occupied frequency band
TETRA	Professional mobile communication system based on digital TDMA technology	Spatial and direct mode space interfaces	851–866, 806–821 MHz
CBTC	Train automatic control system based on wireless communication	AP and antenna	2.412–2.484 GHz
PIS	Service system that provides passengers various types of information	AP and antenna	5.725–5.865, 2.461–2.483 GHz

2.4 System level electromagnetic compatibility performance test

Apart from interference source search, real performance of the three systems in vehicle-ground and ground-vehicle communication process need to be judged, so that we can find out the optimal mode, with which service quality will not dramatically drop when faced with interference. Conversely, frequency band occupancy problem was paid much attention in our test, because we regard cochannel interference as poor performance culprit.

For research integrity, we made an attempt to take all possible modes into consideration. It consumed time because of lack of prior experience; however, we insisted on completing our goal and managed finally. We also need to say that experimental devices were chosen

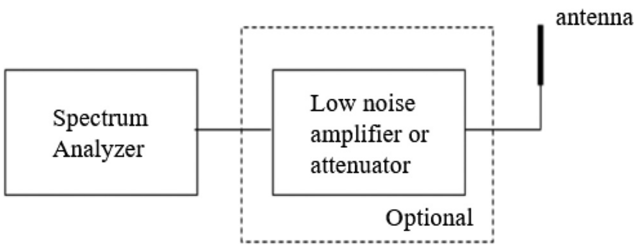

Figure 3.
External interference test equipment setup

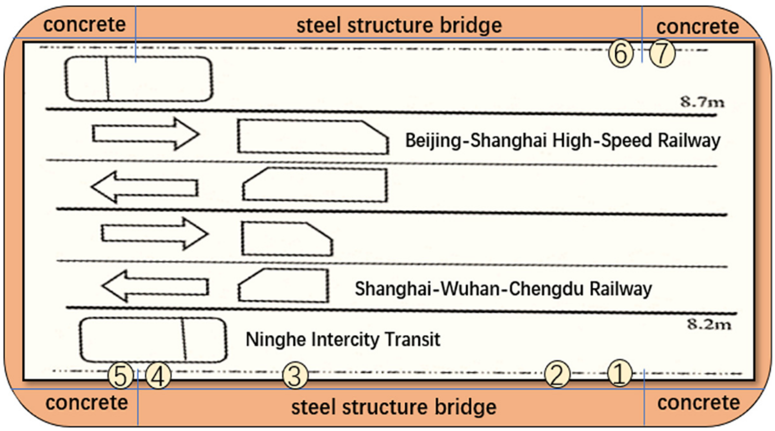

Figure 4.
Test points distribution

Figure 5.
Satellite image of Beijing–Shanghai High-Speed Railway, which is taken from Google map

according to standards or protocols, such as GB50382-2006 and IEEE 802.11 wireless LAN protocol group, so the experimental data was reliable. They were classified into two categories to achieve two-way communication.

Here is a list of main simulated modes that the three communication systems applied:

(1) TETRA: 851–870 MHz (800 MHz) antenna coverage mode.

(2) CBTC: DSSS antenna, DSSS waveguide and FHSS antenna mode.

(3) PIS: 2.461–2.483 GHz (2.4 G) antenna, 5.725–5.865 GHz (5.8 G) antenna and LTE mode.

2.4.1 Bridge deck equipment. On the main bridge, the mode-related antenna and access point (AP) were installed in the following order (Figure 6), so that the three systems could work, respectively. In detail, seven sets of CBTC (DSSS) devices stood at points 2, 4, 6, 8, 10, 12 and 14 beside the track; three sets of CBTC (FHSS) devices were located at points 2, 4 and 6 beside the track; CBTC (waveguide) was placed in the line section from points 2–4; only one TETRA and PIS (TD-LTE) were deployed, the antenna (or transmitting device) of which was located at point 1; seven sets of PIS (a/g) stood at points 3, 5, 7, 9, 11, 13 and 15 alongside

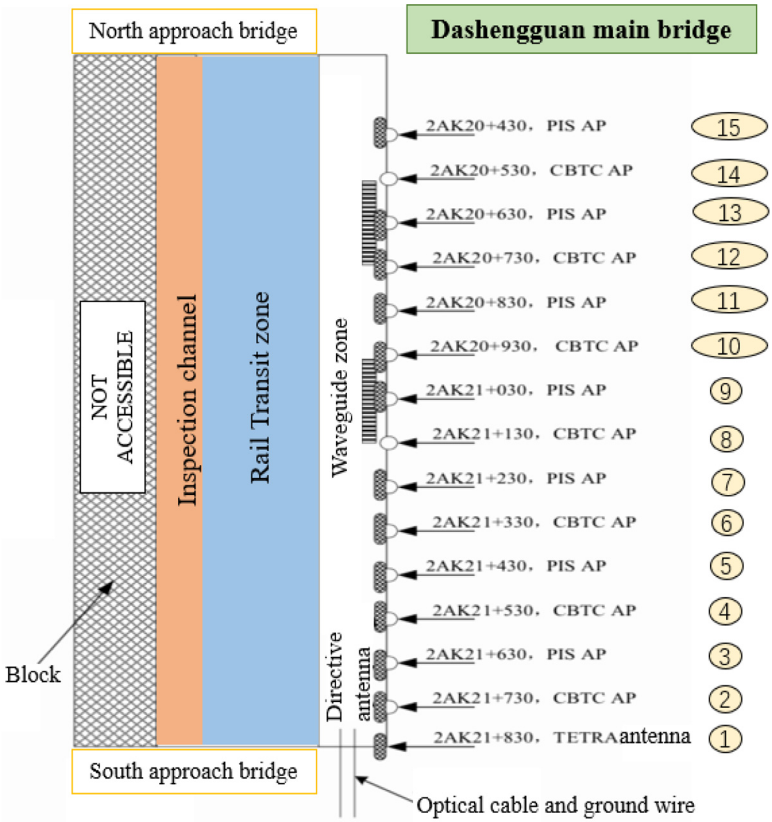

Figure 6.
Antenna and AP equipment installation locations

the track. In addition, point 1 was located at the bridgehead on the east bank, other points were arranged every 100 m westward.

Then changing view to dead ahead of Ninghe Intercity Transit (Figure 7), we could see that both trackside AP and vehicle AP were mounted on the metal bridge deck below the cable bracket, while the crack waveguide was placed on the metal platform.

The bridge deck equipment communicated with ground devices via fiber optic cable successfully in our test. We intended to generalize AP layout reference method, by which the three systems could work, respectively.

2.4.2 Ground equipment. Figure 8 depicts the ground equipment, which includes one test server, one ground server, a TETRA base station, switches and power supply equipment. We installed the devices in rentals or makeshift houses.

2.4.3 Equipment collaboration. With collaboration between bridge deck and ground equipment, the overall test equipment installation was accomplished. Figure 9 exhibits the transmission way of the three communication systems, that is, TETRA antenna is

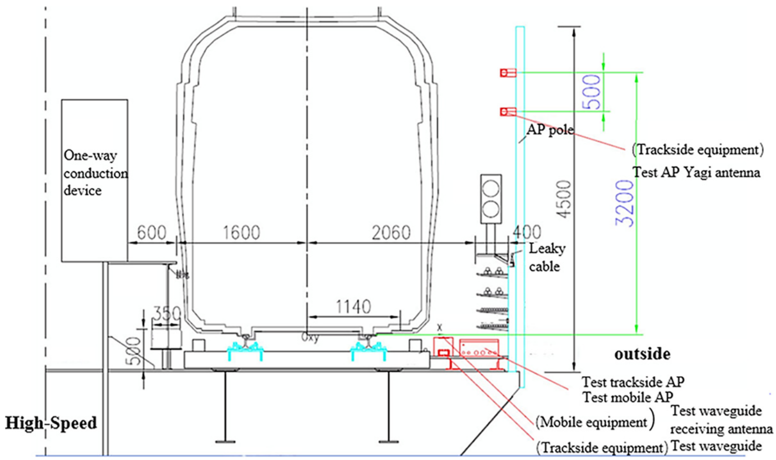

Figure 7.
Equipment arrangement diagram

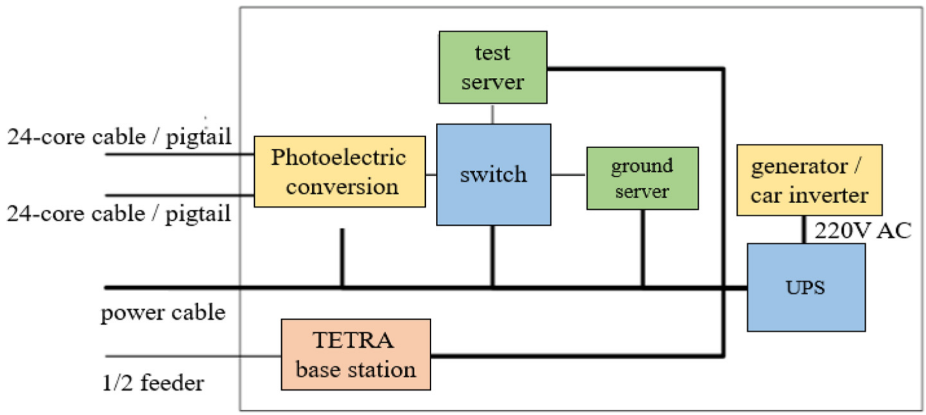

Figure 8.
Ground equipment installation

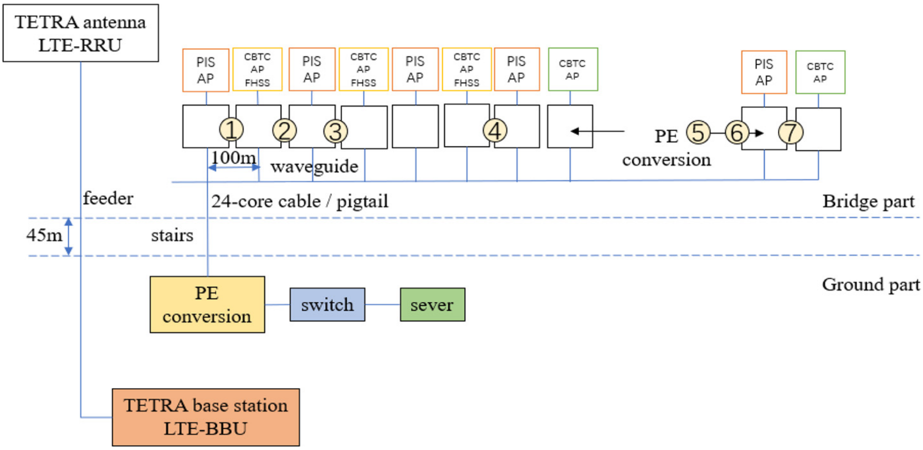

Figure 9.
Overall layout of the performance test system

controlled by the ground base station; LTE-RRU and BBU is a group; signals from CBTC and PIS AP can be recognized through photoelectric conversion; and seven test points are also marked. Finally, the whole system was put into use and got satisfying effect.

3. Tests and results

We conducted simulations on the platform we established. We also adjusted the selected points after each test for accuracy, so that the effects of random factors on the test results could be avoided. Totally, we collected data from 14 test points of three experiments, which costs one and a half year. Finally, we obtained a sufficient number of test samples and here are the results.

3.1 External interference test and interference comparison test

3.1.1 Tetra test. Figure 10 shows the widest interference band of TETRA at point 3, that is, only 806.4–807.6, 808.8–810.2, 810.6–811.6, 812.6–817.0 and 817.4–821.0 MHz of up-band and 851.8–852.2 and 856.8–859.2 MHz of down-band were immune to interference. After overall consideration from seven test points, the most suitable frequency band was intended to be 812.6–814.2 and 857.6–859.2 MHz, where existed no signal at all.

Then the comparison test was launched and indicated when Beijing–Shanghai High-Speed Railway passed by, interference signals occasionally were generated but not in fixed band. Figure 11 demonstrates the interfered band at points 4 and 7, which was 827.0–830.0, 832.4–834.6, and 894.0–896.4, 898.6–899.6 MHz. However, maximum interference level was only −88.09 (833.0 MHz) and −83.80 dBm (899.2 MHz), less than −80 dBm.

3.1.2 CBTC test. In practice, CBTC frequency band is divided into 11 channels for signal transmission. Thus, four points (points 1, 3, 4, 6) were selected to detect the number of access devices and maximum interference level of each channel, presented in decibels. Table 2 lists the external interference test results for CBTC.

Figure 12 is the typical result for CBTC interference comparison test. The interfered band at test point 3 was 2400.0–2405.8 MHz, while maximum level equaled −90.51 dBm (2402.0 MHz), which was very narrow. And there existed even no interference at test point 7.

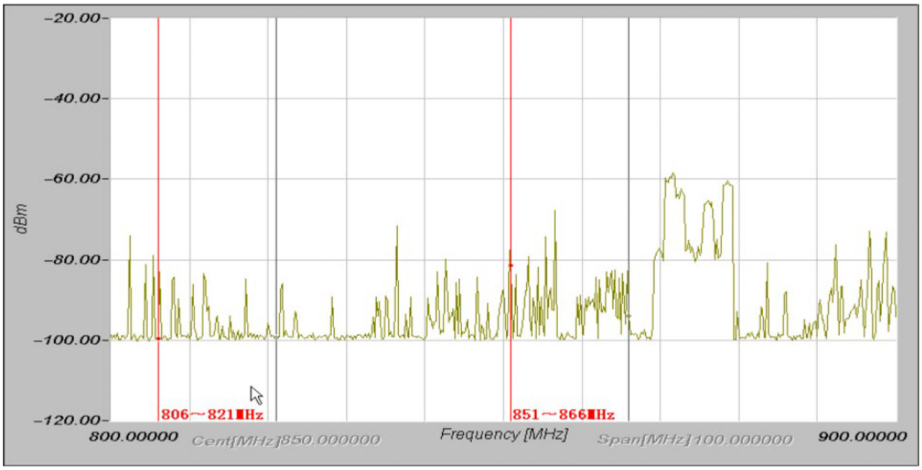

Figure 10.
TETRA external interference test result at point 3

Nevertheless, the spectrum of point 6 exhibited "glitch" moment, as shown in Figure 13. The interfered band extended to be 2455.4–2456.2, 2457.2–2458.0 and 2458.6–2459.2 MHz, however, the signal power was only about −80 dbm.

3.1.3 PIS test. PIS external interference test demonstrated that there was no signal at any test point under normal conditions, nor interference emerged in this band (5.8 GHz) when Beijing–Shanghai High-Speed Railway was passing by.

3.2 System level electromagnetic compatibility performance test

3.2.1 Tetra performance test. Since communication system's reliability is crucial, we chose bit error ratio (BER) to find out to what degree TETRA can be disturbed. The results were listed in Table 3.

When a train of Beijing–Shanghai High-Speed Railway was passing by, BER increased, and no call dropped throughout the testing process.

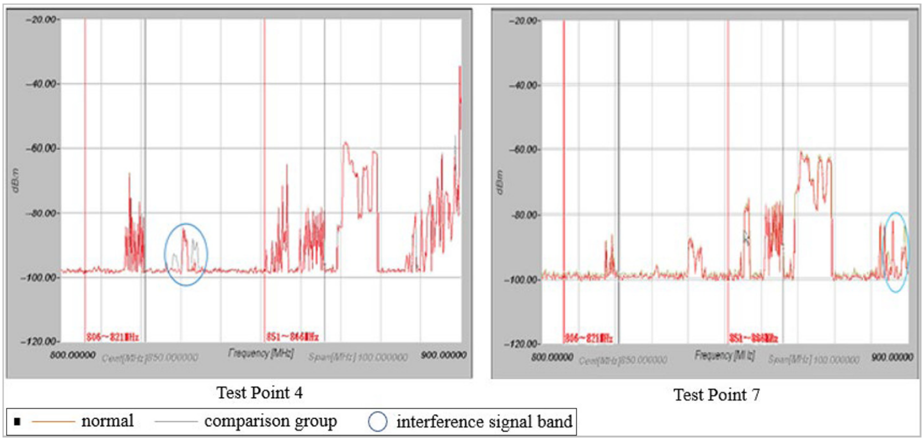

Figure 11.
TETRA interference comparison test results at points 4 and 7

Table 2.
CBTC external interference test results

Channel frequency (MHz)	Test point 1 AP number	Test point 1 Maximum level (dBm)	Test point 3 AP number	Test point 3 Maximum level (dBm)	Test point 4 AP number	Test point 4 Maximum level (dBm)	Test point 6 AP number	Test point 6 Maximum level (dBm)
2,412	8	−80	5	−81	6	−80	3	−89
2,417	0	−81	1	−86	1	−81	0	N/A
2,422	1	−80	0	−92	0	−80	0	N/A
2,427	1	−83	0	−92	0	−83	0	N/A
2,432	1	−83	1	−83	2	−83	0	−87
2,437	3	−80	4	−82	0	−80	2	−89
2,442	1	−81	0	−82	2	−81	0	N/A
2,447	0	−87	0	N/A	0	−87	0	N/A
2,452	0	N/A	0	−94	0	N/A	0	−91
2,457	0	−82	2	−85	1	−82	0	N/A
2,462	6	−81	3	−81	5	−81	2	−90

3.2.2 CBTC performance test. CBTC's performance need to be evaluated under different modes. We chose transmission throughput, delay and packet loss rate as vital indicators.
3.2.2.1 DSSS antenna redundant and nonredundant mode. The first test object was DSSS antenna, during the test, device configuration followed 802.11 b and transmit power equaled 15 dBm. Table 4 lists results at points 3 and 7.

3.2.2.2 DSSS waveguide mode. Under DSSS waveguide mode, the antenna hanging height was 40 cm. Device configuration and the transmit power were the same with those of DSSS antenna mode (Table 5).

3.2.2.3 FHSS antenna mode. Under FHSS antenna mode, the configuration turned to be frequency hopping and transmit power equaled 10 dBm. The results were concluded in Table 6.

3.2.3 PIS performance test. PIS occupies frequencies in 2.4 GHz or 5.8 GHz, and both of them are built in mesh mode (Kuang and Liu, 2017), so we selected three test channels to compare PIS antidisturbance performance within different frequency bands (Table 7). During the test, dynamic control was applied.

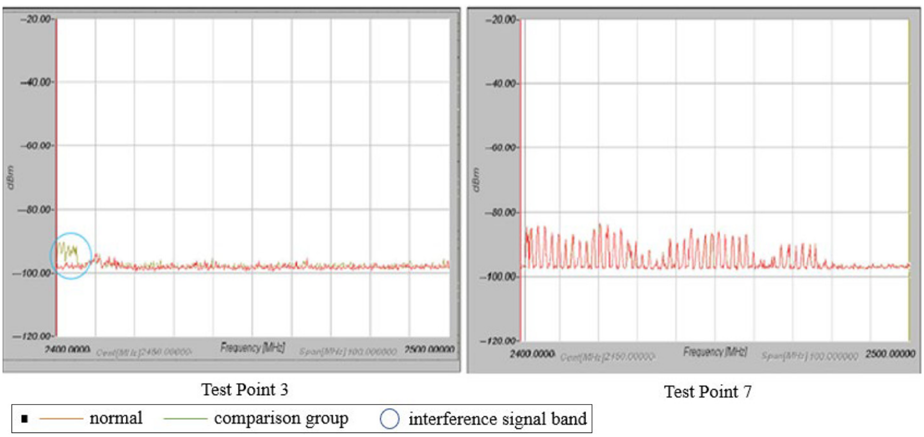

Figure 12.
CBTC interference comparison test results at points 3 and 7

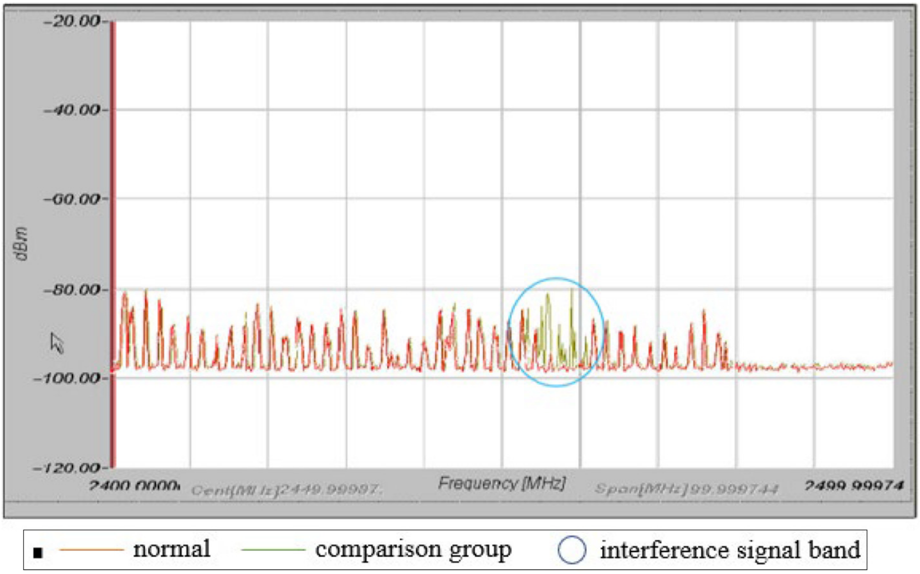

Figure 13.
CBTC interference comparison test result at point 6

Then we adopted PIS LTE mode, as mentioned in Tang *et al.* (2016). We set RSSI at points 3 and 7 as −49 and −73 dBm, respectively, otherwise field strength coverage from a distance farther than 1 km turned so weak that results might get distorted. For the same purpose, the one-way packet loss rate was also tested under different throughput, that is, 1 Mbps and 400 Kbps, respectively.

As depicted in Figure 14, both vehicle-ground and ground-vehicle process went well. When a high-speed train passing on the Beijing–Shanghai Railway tracks, the vehicle-ground one-way throughput reached 6.629 and 4.048 Mbps, 0.02 and 0.1 Mbps higher than the throughput in normal conditions, which means the throughput did not reduce at all. Moreover, response time did not increase and no packet loss took place at any test point.

Test item	TETRA	Test channel	851.250 MHz
Device configuration	Country code 460 Network code 888 Group No. 10011001–2	Test method Transit power	group call (30 s) 36 dBm
	Normal		Railway passed
Test location: test point 5; weather condition: small thunder shower			
Field strength (dBm)	−84		−85
BER (%)	0		1
Test location: test point 6; weather condition: sunny			
Field strength (dBm)	−87		−87
BER (%)	2.2		2.8
Test location: test point 7; weather condition: cloudy			
Field strength (dBm)	−88		−88
BER (%)	2.8		3

Table 3.
TETRA performance test results

Table 4.
Results of CBTC performance test under DSSS antenna mode

Mode: redundant	Test location: test point 3 Weather condition: cloudy		Test location: test point 7 Weather condition: light rain	
Condition	Normal	Railway passed	Normal	Railway passed
Field strength (RSSI; dBm)	−41, −67	−41, −67	−66, −66	−41, −67
S/N (dBm)	−96	−96	−96	−96
Throughput (Mbps)	5.458	5.401	4.995	4.756
Delay (ms)	3	3	3	3
Packet loss rate (%)	0.004	0.01	0.06	0.06
Mode: nonredundant	Test location: test point 3 Weather condition: cloudy		Test location: test point 7 Weather condition: light rain	
Condition	Normal	Railway passed	Normal	Railway passed
Field strength (RSSI; dBm)	−67	−85	−66	−66
S/N (dBm)	−96	−96	−96	−96
Throughput (Mbps)	2.423	3.173	4.242	4.084
Delay (ms)	7	7	4	4
Packet loss rate (%)	7.37	15.79	0.66	0.82

Table 5.
Results of CBTC performance test under DSSS waveguide mode

	Test location: test point 2; weather condition: light rain	
Condition	Normal	Railway passed
Field strength (RSSI; dBm)	−48, −66	−48, −66
S/N (dBm)	−96	−96
Throughput (Mbps)	1.808	1.808
Delay (ms)	9	9
Packet loss rate (%)	0.00	0.09

Table 6.
Results of CBTC performance test under FHSS antenna mode

	Test location: test point 1; weather condition: sunny	
Condition	Normal	Railway passed
Field strength (RSSI; dBm)	−65	−65
S/N (dBm)	−96	−96
Throughput (Mbps)	5.739	5.909
Delay (ms)	7	7
Packet loss rate (%)	0.06	0.06

3.2.4 CBTC and PIS mutual interference test. If 2.4 GHz PIS is preferred, it will occupy part of channels that CBTC use. Hence, we desire to find out to which extent the two systems influence each other. Table 8 concludes their independent test results at point 2, in which channel of CBTC were 11 and 1, while PIS channel was 1.

Then in full load condition, the throughput of CBTC and PIS were recorded as Figure 15. It implies that CBTC throughput reached 5.062 Mbps, while PIS performance was bad, dropping to 28.728 Mbps. Next, we turned CBTC to light load mode, and traced out PIS performance. We can easily read from Figure 16 the PIS packet loss rate as well as delay decrease.

4. Discussions

We further analyzed the experiment results to summarize practical recommendations that communication systems would take in such complex environment. The following sections include data processing and empirical formula supporting.

4.1 External environment and additive factor analysis

4.1.1 External environment analysis. Through external interference test, we learned that the best frequency band for TETRA was 812.6–814.2 and 857.6–859.2 MHz.

Test location	Test point 4		Test point 1		Test point 3	
Weather	Cloudy		Sunny		Cloudy	
Test channel	11 (2.4 GHz)	11 (2.4 GHz)	149 (5.8 GHz)	149 (5.8 GHz)	6 (2.4 GHz)	6 (2.4 GHz)
Condition	Normal	Railway passed	Normal	Railway passed	Normal	Railway passed
Field strength (dBm)	−51	−51	−77	−77	−81	−81
S/N (dBm)	−97	−97	−97	−97	−97	−97
Throughput (Mbps)	29.081	29.243	13.217	20.273	13.217	10.465
Delay (ms)	7	3	39	40	4	5
Packet loss rate (%)	0.22	0.18	6.16	6.56	0.67	0.71

Table 7. PIS performance test results

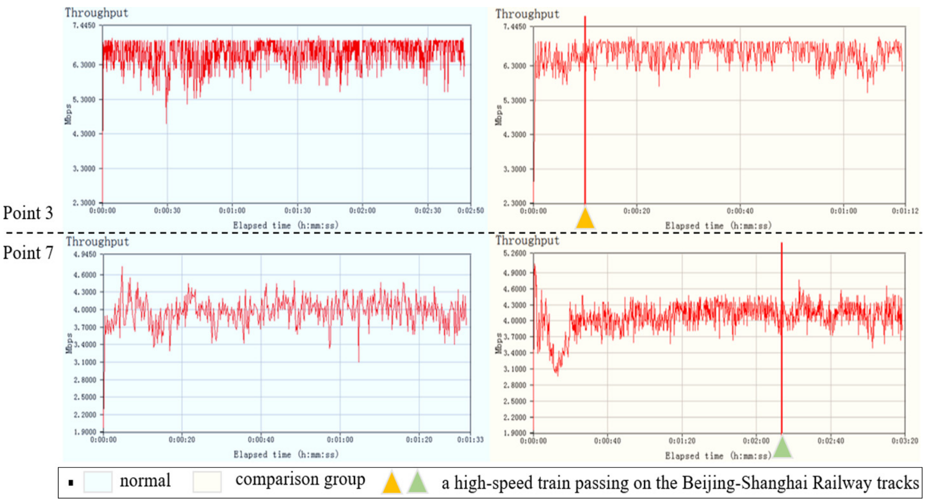

Figure 14. Results of CBTC performance test under LTE mode

Item	CBTC(11,1)	PIS(1)
Field strength (dBm)	−35, −48	−67
S/N (dBm)	−96	−97
Throughput (Mbps)	4.94	43.174
Delay (ms)	4	4
Packet loss rate (%)	0.06 (pressure: 800Kbps)	0.14 (pressure: 800Kbps)

Table 8. CBTC and PIS independent performance test result

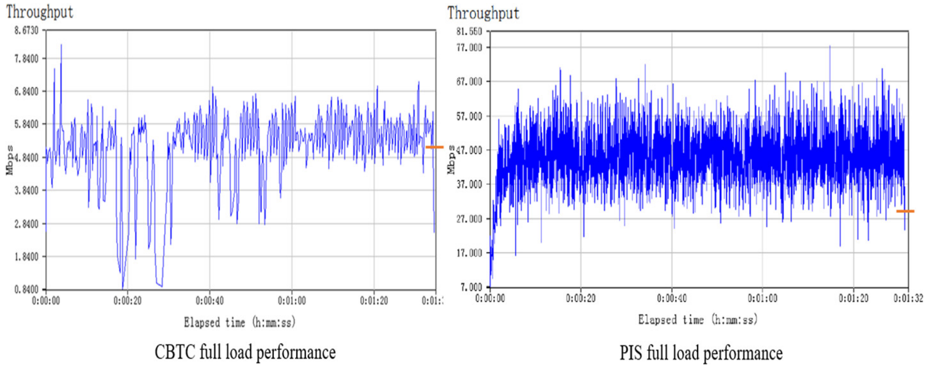

Figure 15.
CBTC and PIS full load test result

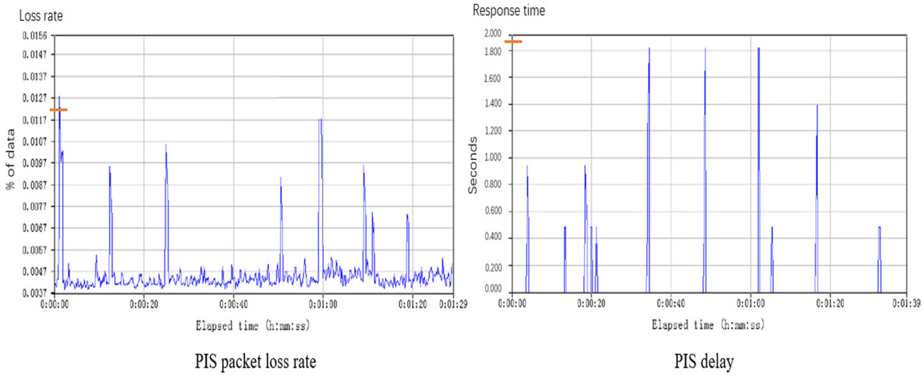

Figure 16.
PIS packet loss rate and delay under CBTC light load

For CBTC, maximum power in each channel was less than −80 dBm, although the exact values in corresponding and adjacent channels rose when more access devices joined in the system. And moreover, AP number and maximum interference level of the system exhibited the same tendency, as shown in Figure 17, which exemplifies results at point 3.

4.1.2 Multirails environment. Compared with those in normal conditions, performances of three communication systems usually experienced reduction when a high-speed railway passed by. However, the change was not so huge as to cause abnormal signal transmissions. Specifically speaking, TETRA and PIS were not interfered at all. While for CBTC, “glitch” phenomenon emerged at point 6, but the probable interference source was the nearby WLAN signal used in FHSS rather than the adjacent track.

Hence, we hypothesize that the insignificant interferences owe to adequate distances between the tracks, and here is the theoretical verification: to decrease interference, autotransformer power-supply mode has been adopted by Beijing–Shanghai High-Speed Railway and Shanghai–Wuhan–Chengdu Railway, so that the Dashengguan overhead line is a four-wire system. The distances between the four lines and our experimental objective (Ninghe Intercity Transit communication cable) were measured to be 7.9, 12.9, 22.9, 27.9 m, respectively.

4.1.2.1 Magnetic hazard potential. Under normal operating conditions, it can be described as equation (1):

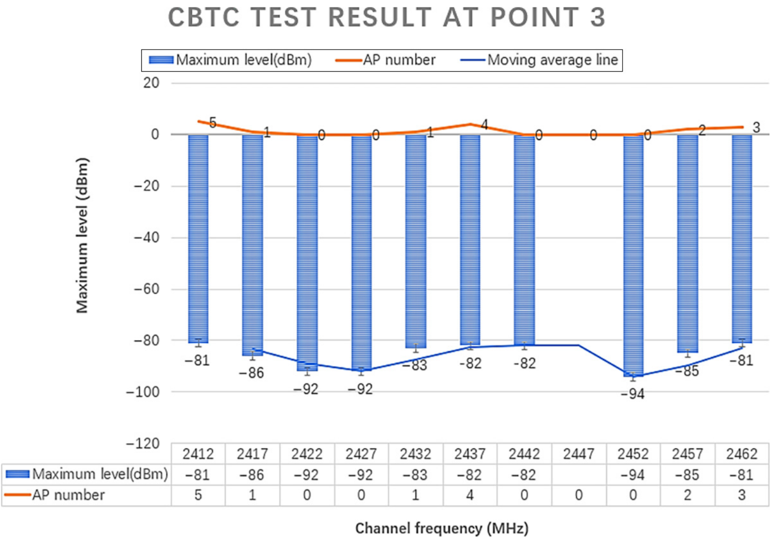

Figure 17. CBTC AP and maximum level at point 3

$$E = \sum_{i=1}^{N} \omega M_i I_{pi} I_d \lambda \, TK, \tag{1}$$

where M_i is the ith mutual inductance coefficient between overhead lines and the communication cable at 50 Hz; I_p = 3.7 km is the approximate bridge span; I_d = 1,200 A is the equivalent traction current of overhead contact network; λ, T, K are the rail shielding factor, the communication cable shielding coefficient, and the magnetic integrated shielding coefficient of ground conductor.

The potential turns out to be 26.73, 23.463, 18.117, 16.335 V, so E = 36.19 V according to superposition method. Obviously, E is under maximum 100–150 V. Considering about short circuit faults, I_s = 20–30 kA replaces I_d, so the potential is calculated to be 668.327, 586.64, 452.98, 408.42 V. Thus ≈ 1,078.33 V, which is also less than 1,080 V.

4.1.2.2 Telecommunication lines interference voltage [equation (2)].

$$U_e = \sqrt{\frac{600}{Z_c}} \cdot \pi f_e M_e I_{pr} \lambda_e S_e t_e \eta_e l_p \times 10^3, \tag{2}$$

where:

$$I_{pr} = I_Z K_1 K_{m2} K_f \tag{3}$$

In equation (3), I_{pr} is the equivalent interference current at 800 Hz; I_z is the total load current of overhead contact network; Z_c = 600 Ω is the characteristic impedance of the communication line.

M_e equals 330, 250, 160, 120 μH/km; U_e equals 0.081, 0.0619, 0.0396, 0.0297 mV. Thus, E = 0.113 mV, much less than the maximum interference value.

Therefore, as long as the space between the overhead wire and communication cable is more than 8 m, the surrounding electromagnetic environment is basically good. It holds up in Dashengguan section for the shortest track distance equals 8.2 m (between Ninghe Intercity Transit uplink and Beijing–Shanghai High-Speed Railway). Moreover, if the lines are shielded by rows of trees, absorption apparatus, etc., the electromagnetic radiation influence will be much smaller.

4.1.3 Additive factor analysis. Figure 18 explains that during TETRA performance test (take TETRA as an example), BER at point 7 reached 3%, while at point 5, it was only 1%. However, the latter growth rate was bigger when a railway passed by. It means TETRA performance is closely related to field strength. Like point 7, signals were weakened by the bridge's shielding effect there, so its service quality degraded.

In addition, our research proves no obvious relevance between the communication system performance and weather condition, and moreover, the shielding effects of steel as well as concrete structure on field strength are on the whole the same.

4.2 Mode comparison

4.2.1 CBTC mode selection. CBTC mode selection is regarded as research emphasis during the system level performance test, on account of its transform convenience.

Table 9 lists CBTC performance under antenna redundant and nonredundant mode at points 3 and 7. When a high-speed railway was running on the close track, the short-term throughput decreased under redundant mode, and delay was 3 ms. However, switching to the nonredundant mode, CBTC throughput experienced significant growth at point 3, which attributed to available bandwidth reduction caused by received signal strength drop. Then we closed neighboring AP at point 7, the field strength turned out to be stable. Nevertheless, packet loss rate under nonredundant mode still increased when CBTC was interfered.

Next, we make a comparison between two modes, throughput shrank in nonredundant condition, meanwhile, response time (delay) and packet loss rate had significant growth. Thus, we deem that CBTC performs better to some extent under antenna redundant mode.

Furthermore, CBTC had very low packet loss rate under waveguide mode in our test, which validates waveguide application advantages. While under FHSS mode, CBTC throughput was constant, and the loss rate could also be accepted. However, WLAN signals from FHSS devices might interfere with CBTC. Therefore, CBTC DSSS waveguide mode is preferred.

4.2.2 PIS mode selection. PIS also has two commonly used modes, namely, the mesh mode and LTE mode. We tested PIS performance under mesh mode within 2.4 and 5.8 GHz frequency bands, and found more than once that secondary interference was involved in the

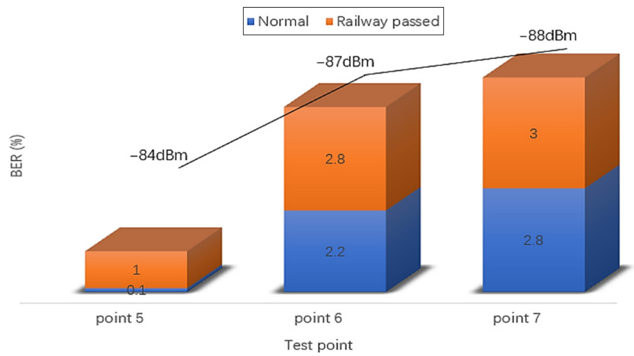

Figure 18.
TETRA performance test results

vehicle-ground communication wireless channel when Beijing–Shanghai High-Speed Railway passed by.

In comparison, PIS under LTE mode was much more stable: almost no delay was detected in the system level performance test. It should conform to characteristics of LTE, that is, the dedicated frequency band and interference rejection combining technology (Liu *et al.*, 2016).

To sum up, appropriate modes should be selected for different needs, so that communication systems can work even well.

4.3 Frequency band usage

4.3.1 PIS 2.4 GHz versus 5.8 GHz. Nowadays, 5.8 GHz PIS gains the popularity among scholars, because it contains abundant information and is able to meet the high requirements of wireless communication. However, we need to take interference level into account, for the equal importance of communication quality. Our test supplemented that 5.8 GHz PIS experienced a larger attenuation than PIS with 2.4 GHz frequency band, that is to say, the response time and packet loss rate grew a lot when interference emerged. Thus, we should judge the two frequency bands more comprehensively.

4.3.2 CBTC and PIS-shared system. If PIS system occupies 2.4 GHz frequency band, cochannel interference will emerge when it works together with CBTC. The independent performance test showed that PIS throughput was nearly tenfold of CBTC throughput, and the PIS packet loss rate was a little higher. Then the frequency-sharing test was conducted, as a comparison. It indicated that CBTC performance did not decreased significantly, for channel 11 was only occupied by CBTC, so that CBTC could maintain normal operation. While performance of PIS dropped a lot. Finally, we changed CBTC to light load, delay and loss rate decreased to normal level again. Hence, PIS is considered normal when CBTC only does its basic job.

The result implied that if two communication systems share the same channel, performances will turn worse. The assumptions can be verified as follows.

The channel overlap interference degree can be described by interference factor $|spec(f)|^2$, and the power spectrum density of OFDM signal is the sum of power spectrum subdensity on N subcarrier [equation (4)]:

$$|spec(f)|^2 = \frac{1}{N}\sum_{i=0}^{N-1}\left|T\frac{\sin(\pi(f-f_i)T)}{\pi(f-f_i)T}\right|^2 \tag{4}$$

Test location	Test point 3		Test point 7	
Weather condition	Cloudy		Light rain	
Condition	Normal	Railway passed	Normal	Railway passed
Throughput (r; Mbps)	5.458	5.401	4.995	4.756
Throughput (n-r; Mbps)	2.423	3.173	4.242	4.084
Difference (Mbps)	−3.035	−2.228	−0.753	−0.672
Delay (r; ms)	3	3	3	3
Delay (n-r; ms)	7	7	4	4
Packet loss rate (r; %)	0.004	0.01	0.06	0.06
Packet loss rate (n-r; %)	7.37	15.79	0.66	0.82

Table 9.
CBTC mode comparison result

The OFDM signal can be affected by filter of IEEE802.11 standard wireless network, thus, the power spectrum density should greatly reduce. Moreover, IF filter frequency response function can be described as equation (5):

$$Filt(w) = \frac{1}{1 + (2.6w)^6} \tag{5}$$

where ω is the angular frequency (18). Hence, the overlap of two channels at a specified frequency is calculated as equation (6):

$$overlap(i,j,f) = spec(ch(i,j)) \cdot Filt(ch(i,f)) \cdot spec(ch(i,j)) \cdot Filt(ch(j,f)), \tag{6}$$

where

$$ch(i,j) = \frac{f - 2412 - 5(i-1)}{22}.$$

This function can be integrated for a certain frequency band, and then we will obtain the interference factor between the two channels, namely, $olf_{i,j}$. It verifies that cochannel interference really exists.

5. Conclusions

This study gains valuable information from three integral tests: external interference test for communication systems working on characteristics identification; interference comparison test confirming main disturbance factors; and system level electromagnetic compatibility performance test considering the overall performance of three communication systems (TETRA, CBTC and PIS), so as to dig into underlying principles. Through unremitting efforts, our one-to-one scale analog equipment installation method can also be extended to other projects, including sites where communication devices are especially intricate. After scientific analysis, we make following conclusions:

- External EMI has no obvious influence on main functions of urban rail transit communication systems, as long as the field strength coverage stays good.
- A high-speed passing railway can create large electromagnetic field, and AC traction devices can affect DC operation, resulting in communication equipment malfunction, etc. But an enough distance, 8 m or more, between a passing railway and the tested transit can keep the communication system from being influenced. Plus, the electromagnetic hazard under normal or short-circuit fault conditions are acceptable.
- The performance of urban rail transit communications is not related to bridge materials or weather conditions. Furthermore, appropriate electromagnetic shielding measures, such as rows of trees along the track and protection over communication cables, can suppress the shielding effect.
- Different communication modes may present various performances: DSSS waveguide and LTE mode are more stable for CBTC and PIS.
- It is better that CBTC and PIS do not share a same frequency band, otherwise communication quality will reduce due to cochannel interference.

Our approach, including experiment setup and theoretical analysis, successfully helped us find out crucial facts of EMI on communication systems. Given the pioneering structure and load of the Nanjing Dashengguan Bridge, our study also provides convincible recommendations and solid reference to other complex rail transit systems.

References

Ahmad, I., Chen, W. and Chang, K. (2017), "LTE-railway user priority-based cooperative resource allocation schemes for coexisting public safety and railway networks", *IEEE Access*, Vol. 5, pp. 7985-8000, doi: 10.1109/ACCESS.2017.2698098.

Flyvbjerg, B. (2005), "Measuring inaccuracy in travel demand forecasting: methodological considerations regarding ramp up and sampling", *Transportation Research Part A: Policy and Practice*, Vol. 39 No. 6, pp. 522-530.

Flyvbjerg, B. (2007), "Cost overruns and demand shortfalls in urban rail and other Infrastructure", *Transportation Planning and Technology*, Vol. 30 No. 1, pp. 9-30, doi: 10.1080/03081060701207938.

Heddebaut, M., Deniau, V., Rioult, J., *et al.* (2017), "Mitigation techniques to reduce the vulnerability of railway signaling to radiated intentional EMI emitted from a train", *IEEE Transactions on Electromagnetic Compatibility*, Vol. 59 No. 3, pp. 845-852.

Jun, Y., Yang, L., Bo, C., *et al.* (2016), "External electromagnetic turbance test and suppression measures for 350 km h-1 standardized EMU in China", *China Railway Science*, Vol. 37 No. 6, pp. 135-140, doi: 10.3969/j.issn.1001-4632.2016.06.18.

Kuang, X. and Liu, L. (2017), "WLAN system performance of PIS and CCTV services based on field test results in 5.2GHz and 5.8GHz", *2017 Chinese Automation Congress (CAC)*, *Jinan*, pp. 4374-4377. doi: 10.1109/CAC.2017.8243549.

Kui, X., Menglin, X. and Yawei, W. (2015), "Application of electromagnetic compatibility rapid test technology for wireless receiver in complex electromagnetic environment", *Journal of Astronautic Metrology*, Vol. 35 No. 5, pp. 21-26, doi: 10.3969/j.issn.1000-7202.2015.05.007.

Li, W., Wei, G., Pan, X., Wang, Y., Wan, H. and Sun, S. (2017), "Interference prediction method for communication equipment in complex electromagnetic environment", *Journal of Electronics and Information Technology*, Vol. 39 No. 11, pp. 2782-2789, doi: 10.11999/JEIT170107.

Liu, F., Zhao, H., Quan, X., *et al.* (2016), "Eigen domain interference rejection combining algorithm for MIMO systems", *IEEE Communications Letters*, Vol. 20 No. 5, pp. 850-853.

Mingyang, C. (2014), "Research on the impact of electromagnetic induction when urban rail transit crossing the Yangtze River via the Dashengguan Bridge of the high-speed railway", Beijing Jiaotong University, Beijing.

Nan, Y. (2017), "Simulation analysis of induced voltage absorption on Ninghe Intercity Dashengguan Bridge", *Electronic Technology and Software Engineering*, (023).

Peng, Z. (2015), "Research on coexistence of Nanjing Metro airport line CBTC and PIS in 2.4G frequency band", *China Science and Technology Information*, Vol. 18, pp. 50-51, doi: 10.3969/j.issn.1001-8972.2015. 18.015.

Pous, M., Azpúrua, M.A., Oliva, J.A., Aragón, M., González, I. and Silva, F. (2018), "Full time domain EMI measurement system applied to railway emissions according to IEC 62236-3-1/EN 50121-3-1 Standards", *2018 International Symposium on Electromagnetic Compatibility (EMC EUROPE)*, *Amsterdam*, pp. 260-265, doi: 10.1109/EMCEurope.2018.8485173.

Tang, T., Dai, K., Zhang, Y., Zhao, H. and Jiang, H. (2016), "Field test results analysis in urban rail transit train ground communication systems of integrated service using LTE-M", *2016 IEEE*

19th International Conference on Intelligent Transportation Systems (ITSC), *Rio de Janeiro*, pp. 2017-2021, doi: 10.1109/ITSC.2016.7795882.

Xiwei, L. and Feng, Z. (2014), "Measurement and analysis of wayside EMI on Wuhan-Guangzhou high-speed electrical railway", *Railway Standard Design*, Vol. 58 No. 9.

Zhang, B., Xie, J., Wang, Z., Yang, J. and Yan, H. (2018), "Research on power-frequency electromagnetic interference model of multicore twisted signal cable of high-speed railway", *Turkish Journal of Electrical Engineering and Computer Sciences*, Vol. 26 No. 4, pp. 2077-2087, doi: 10.3906/elk-1712-169.

Further reading

Shen, L. and Dongxiang, L. (2017), "Research on WLAN interference problem of PIS and CBTC coexistence", *Electronic Test*, Vol. 2, pp. 58-60, doi: 10.3969/j.issn.1000-8519.2017.02.031.

Corresponding author

Xiaowen Liu can be contacted at: 2031335@tongji.edu.cn